RM L55C16

NACA RM L55C16

NACA

RESEARCH MEMORANDUM

EFFECT OF SEVERAL MODIFICATIONS TO CENTER BODY AND COWLING ON SUBCRITICAL PERFORMANCE OF A SUPERSONIC INLET AT MACH NUMBER OF 2.02

By Robert L. Trimpi and Nathaniel B. Cohen

Langley Aeronautical Laboratory
Langley Field, Va.

NATIONAL ADVISORY COMMITTEE
FOR AERONAUTICS

WASHINGTON

May 20, 1955
Declassified October 16, 1961

NACA RM L55C16

NATIONAL ADVISORY COMMITTEE FOR AERONAUTICS

RESEARCH MEMORANDUM

EFFECT OF SEVERAL MODIFICATIONS TO CENTER BODY AND COWLING ON SUBCRITICAL PERFORMANCE OF A SUPERSONIC INLET AT MACH NUMBER OF 2.02

By Robert L. Trimpi and Nathaniel B. Cohen

SUMMARY

Several modifications of the center body and cowling of a supersonic inlet at a Mach number of 2.02 and angles of attack up to $12\frac{1}{4}^\circ$ have been investigated.

For a conical center body with a subsonic diffusion rate roughly equivalent to that of a 1° included-angle conical diffuser and with cowling-position angle equal to conical-shock angle, use of boundary-layer bleed resulted in a stable range as much as 8 percent greater at angle of attack α than for the configuration without bleed (for which the stable range was negligible) and in an increase of 7 percent in maximum pressure recovery at $\alpha = 12\frac{1}{4}^\circ$.

When the cowling-position angle was 2.4° less than conical-shock angle, the use of boundary-layer bleed resulted in a stable range approximately 12 percent greater than that of the inlet with no bleed over the range of α tested, the stable range being 16 percent at $\alpha = 0^\circ$ and 14 percent at $\alpha = 12\frac{1}{4}^\circ$. With bleed the maximum pressure recovery of the inlet dropped only from 87.4 to 83 percent over an α-variation of $12\frac{1}{4}^\circ$. The performance of this inlet with boundary-layer bleed compared favorably over a range of α with the performance of pivoted-cone and zero-diffusion-rate inlets reported in NACA RM E53I30 and NACA RM E53E26.

At $\alpha = 4^\circ$ and 8°, the use of bleed on only the upper surface of the 25° conical center body had the same effect as the use of bleed over the entire circumference for conditions of shock angle equal to cowling-position angle. When the cowling-position angle was 2.4° less than the shock angle, bleed on only the upper surface resulted in a stable

subcritical range approximately half that obtained with complete bleed. Performance with bleed on only the bottom surface was the same as that found with no bleed.

Use of an eight-fluted center body was ineffective at α as a method of increasing the stable subcritical performance by boundary-layer control. Use of a four-fluted center body, which produced a conical shock distortion at the cowling of six cowling-lip thicknesses, was ineffective as a method of increasing the stable subcritical performance by vortex sheet distortion.

For configurations having a conical center body at $\alpha = 0^{\circ}$, the following trends were noted as the cowling lip was thickened from 0.003 to 0.040 inch: For conical shock on lip with and without bleed, the stable range was always negligible and the peak pressure recovery decreased. For shock ahead of lip and no bleed, the stable range was doubled while the pressure recovery decreased 0.3 percent. For shock ahead of lip and boundary-layer bleed, the stable range was halved and the pressure recovery decreased about 1 percent. The net result of bleed and thickening of the lip in the last case was an increase in stable range from 3 to 15 percent at a thickness of 0.003 inch, from 5 to 16 percent at 0.010 inch, and only from 6.4 to 8.2 percent at 0.040 inch.

INTRODUCTION

The phenomena of buzzing or pulsation of the shock system ahead of an air inlet in supersonic flight has been the subject of many studies since Oswatitsch first noted it in 1944 (ref. 1). Buzzing occurs when either all or part of the inlet shock system, which has been displaced forward from the design position either because of flight at "off design" conditions or maneuvering, reaches an unstable location and begins to oscillate. It has been shown in reference 2 that the instantaneous flow conditions which exist from immediately behind the shock system to just inside the inlet cowling are the determining factors of shock-pattern stability. Boundary-layer separation in this region was proved to be a strong destabilizing influence. For multishock diffusers, another destabilizing influence was the entrance into the cowling of a vortex sheet with concurrent higher entropy air. This vortex sheet results from the coalescence of two shocks into a single stronger shock ahead of the inlet, and its role as a cause of buzz was first reported in reference 3.

The use of a long throat of nearly constant cross section has been successful in extending the stable flow range in certain cases, (refs. 3 and 4). The long throat reduces the adverse pressure gradient inside the cowling and thus retards boundary-layer growth and separation. In cases involving vortex sheets, the long throat also permits gradual mixing of

the different entropy air before subsonic diffusion so that there is appreciable attenuation of the strong destabilizing pressure pulse, which would be created by the entrance of the higher entropy air accompanying the vortex sheet if diffusion were attempted without prior mixing.

Boundary-layer bleed has also been employed as a means of buzz alleviation. Early experiments on conical diffusers at an angle of attack of 0° with boundary-layer-bleed scoops located at about 0.6 and 0.9 of the distance from the cone tip to the cowling were reported in references 3 and 5, respectively. In the latter case, instability was found to occur when the normal or second shock had moved a constant distance in front of the bleed-scoop location irrespective of the cowling-lip position.

An increase in the stable subcritical range at angles of attack was obtained by the use of a pivoted cone which was kept closely alined with the free-stream air flow (ref. 6). Other methods, such as translating the center body and bypassing various amounts of air after it has entered the inlet, have in certain cases been successful in forestalling the advent of buzzing.

The various ways of preventing buzzing mentioned in the previous paragraphs have been successful in many cases, but further investigation is still necessary to explore the possibility of other methods as well as to gain additional information which would permit improved performance, especially at angles of attack. The results of such an investigation for center-body diffusers of conventional and unconventional types with and without boundary-layer bleed are reported in this paper.

SYMBOLS

M	Mach number
m_b	boundary-layer-bleed mass flow
m_o	mass flow at infinity through a stream tube of radius equal to cowling inner radius
Δm	difference between critical (maximum) mass flow and minimum stable mass flow
p_o	average total pressure in ram-jet combustion chamber
p_{o_∞}	total pressure at infinity

R	radial ordinate of cowling or center-body surfaces, in.
R_1	maximum radial ordinate of fluted center bodies
R_2	minimum radial ordinate of fluted center bodies
X	axial distance from cowling lip, in.
x	axial distance from center-body tip, in.
α	angle of attack, deg
θ_l	cowling-position parameter; included angle between axis of ram-jet engine and ray from tip of center body to cowling inner lip, deg
θ_s	angle included between conical shock and axis of ram-jet engine, deg

APPARATUS

Cold-flow tests of "conical" center-body inlets (inlets having center bodies in which the surfaces near the tip are straight lines originating from a common apex) were performed with low-humidity air in a 9- by 9-inch blowdown jet of the Langley Gas Dynamics Branch. The test Mach number was 2.02 ± 0.02, and the test Reynolds number based on maximum internal duct diameter was 5.9×10^6.

A schematic diagram of the experimental model is shown in figure 1 and a closeup of the cowling with a center body in place is shown in figure 2. The center bodies were interchangeable and the value of the cowling-position parameter θ_l could be varied by insertion of spacers. Ordinates for the cowlings and center bodies as well as the boundary-layer slot dimensions are given in tables I and II. Cowling A had a 12.4° internal and 17° external lip angle whereas cowling B had a 13° internal and 17° external lip angle. The cowling-lip thickness was 0.010 inch for cowling B and was varied from 0.003 to 0.040 inch for cowling A, most of the tests being conducted at a 0.010-inch thickness. The center bodies, three of which are shown in figure 3, have stainless steel noses and cores with a plastic shell forming the outer contour behind the nose piece. The boundary-layer bleed slots could be filled with plastic to approximate performance of bodies without bleed. Where either top or bottom slots are said to be closed or open, the annular slot was filled with plastic through an arc of 180° either above or below a horizontal plane through the center-body axis.

Center body 1 (conical) had a 25.2° semicone angle. Center body 2 (eight-fluted) had a 27.6° semivertex angle for the flute ridges and a 22.5° semivertex angle for the flute valleys. The area variation in an axial direction was the same as that of a conical center body of 24.7° semicone angle. Center body 3 (four-fluted) had 45° and 20° semivertex angles which gave an area variation equal to that of a 29.8° semicone-angle conical center body. Center body 4 (not shown in fig. 3) had a nose shape nearly identical to that of center body 1 up to a station about 0.5 inch to the rear of the slots, at which point fairing was introduced to produce maximum center-body diameter at about 1 inch behind the slot. The tip of the nosepiece forward of the slot could be retracted into the body so that the flush boundary-layer slot could also be employed as a scoop bleed with a scoop height of 0.02 inch. For the scoop configuration, θ_l is defined as the angle measured as if the nose were still in the flush slot position since the resultant conical shock, after the interaction of the main conical shock from the retracted tip and the oblique shock from the scoop, is approximately in a position relative to the cowling lip which it would occupy with a flush slot. It should be noted that the radius of cowling B is larger than that of cowling A so that for the same value of θ_l the bleed slots were farther from the inlet plane when cowling B was used.

The various inlet configurations shall be designated by a code numbering system: The first number is the center-body number; the second is the value of the cowling-position parameter; the letters "SO" denote boundary-layer slots open; and the letters "SC" denote boundary-layer slots closed. Unless specific mention is made to the contrary, cowling A, with a lip thickness of 0.010 inch, shall be considered to apply to the inlet. Thus, the designation 1-42.5-SO refers to center body 1 at $\theta_l = 42.5°$, boundary-layer bleed slots open, and cowling A with a lip thickness of 0.010 inch.

After preliminary testing, center bodies 2 and 3 were modified in the region where the cross-sectional profile was in transition from a fluted shape to a body of revolution. Typical cross-sectional profiles before and after modification are shown in figure 4. Preliminary data from the unmodified center bodies indicated poor performance and are not presented. For purposes of nomenclature, unless unmodified is used in designating center bodies 2 or 3, it shall be understood that the modified bodies are those to which reference is made.

The variations of area normal to the average streamline with axial distance for the various configurations are shown in figure 5.

A remote-controlled rotary total-pressure rake consisting of 25 tubes spaced in 3 rows was used in conjunction with static-pressure measurements to obtain pressure distributions in the combustion chamber. These pressures were indicated on mercury manometers.

A calibrated remote-controlled plug valve, the position of which was indicated within 0.0015 inch by means of a Selsyn indicator, permitted variation of the exit-nozzle area during a test. The plug-valve setting was used in conjunction with total-pressure readings to obtain main-duct mass flows. A calibrated total- and static-pressure-tube combination was used to measure the mass flow through the boundary-layer-bleed slots. Visual observation of the flow phenomena was afforded by means of a conventional shadowgraph system.

TEST PROCEDURE

The test procedure may be briefly outlined as follows: The tunnel was started with the plug valve retracted. For a given setting of the plug valve, photographs of the manometer board were taken to show settling-chamber total and model combustion-chamber total and static pressures as well as bleed mass flow. The rake was rotated to provide a complete coverage of the combustion chamber. Shadowgraphs of the inlet flow were obtained. This procedure was repeated as the plug valve was advanced in small increments until the onset of instability was noted by watching the inlet on a continuously illuminated shadow-graph screen. The valve was then retracted and readvanced to a position just before that at which the instability was noted and a record made of the minimum stable mass flow. Some records were also made during low-amplitude buzzing.

DATA REDUCTION

Data reduction was based on an area-weighted method. Inasmuch as the total-pressure tubes were located radially at centroids of equal areas, an average of the total-pressure readings was used as the average total pressure in the combustion chamber. The plug valve had previously been calibrated in terms of such an average total pressure; consequently, the mass flow was evaluated as the product of the average total pressure and a valve constant dependent on the valve setting. Mach numbers in the combustion chamber were determined from the ratios of static pressures to total pressures.

RESULTS AND DISCUSSION

Effect on Stable Range of Boundary-Layer Control on Center Body

Since boundary-layer control on the center body is of prime importance, two methods of control were applied. The first was boundary-layer bleed. A flush slot (with one exception), located so that the foot of the normal shock would reach it only after appreciable inlet mass-flow reduction, was incorporated in the various center bodies. Location of this slot at such a distance ahead of the cowling lip has obvious advantages. First, the amount of boundary layer to be removed is smaller when the slot is located nearer the nose tip. This advantage is further increased when the bleed is ahead of the normal shock since the shock markedly thickens the boundary layer. Such a location also avoids the stability limit found in reference 5, where buzz occurred whenever the normal shock had moved a given distance ahead of the bleed position. Although a scoop slot is generally more effective in amount of boundary layer removed, a flush slot was used in these tests because (a) computations indicated that the flush slot should be capable of removing all the boundary layer existing at that slot if the flow ahead of the slot were assumed to be unaffected by the normal shock, and (b) a comparison with the performance of the fluted models in which the use of scoop bleed would have greatly increased fabrication difficulties was desired.

The second method of boundary-layer control attempted was the use of fluted center bodies in which the conical compression surface was replaced by sharp-edged flutes which faired into a body of revolution inside the cowling. The purpose of the flutes with regard to boundary-layer control at angles of attack was not only to act as vortex generators but also to retard the boundary-layer cross flow. Boundary-layer bleed was employed in the valleys of the flute to remove the thick boundary layer.

The maximum amount of boundary-layer-bleed flow for each center body was the following:

	Boundary-layer bleed, m_b/m_o
Center body 1	0.014
Center body 2	0.018
Center body 3	0.015
Center body 4 (flush slot)	0.008
Center body 4 (scoop slot)	0.013

Boundary-layer bleed.- The effectiveness of boundary-layer bleed may be evaluated from figure 6, which is a plot of pressure recovery against mass flow for several configurations employing center body 1, and figure 7, which is a summary of both the amount of mass-flow reduction attainable before instability and the minimum stable pressure recovery plotted against angle of attack for configurations employing center bodies 1 and 4.

An examination of the summary curves (fig. 7(a)) reveals that, at zero angle of attack, configurations 1-42.5-S0 and 1-42.5-SC (design conditions, conical shock on lip) have no stable subcritical mass-flow range. For this inlet configuration with no bleed, the stable subcritical mass-flow range increases with increasing angle of attack to a maximum of 2 percent of m_o at $\alpha = 8^\circ$ and then decreases to zero at $\alpha = 12\frac{1}{4}^\circ$. The effect of bleed on this inlet configuration is to increase the stable subcritical mass-flow range with increasing angle of attack, up to a maximum of 8 percent at $\alpha = 12\frac{1}{4}^\circ$.

For configurations 1-40.0-SC and 1-40.0-S0 (shock ahead of lip), bleed is more effective in increasing the stable range than it was when $\theta_l = 42.5^\circ$. Configuration 1-40.0-SC has a 5-percent stable range at $\alpha = 0^\circ$ which decreases with increasing angle of attack to a minimum of 1 percent at $\alpha = 8^\circ$ and then increases to 2 percent at $\alpha = 12\frac{1}{4}^\circ$. Bleed increased the stable range at an angle of attack of 0° to 16 percent. For this configuration (1-40.0-S0), the variation of stable range with angle of attack was such as to maintain a constant difference of about 12 percent between the stable mass-flow range with and without bleed over the entire angle-of-attack range investigated.

The use of bleed on center body 1 for $\theta_l = 42.5^\circ$ (fig. 7(b)) resulted in a slight decrease (less than 1 percent) in maximum pressure recovery for angles of attack below 6° and an increase up to 7 percent at an angle of attack of $12\frac{1}{4}^\circ$. The bleed was effective for center body 1 at $\theta_l = 42.5^\circ$ in reducing the fall-off with angle of attack in maximum pressure recovery since the no-bleed maximum pressure recovery dropped from a value of 86.4 percent at $\alpha = 0^\circ$ to 71.7 percent at $\alpha = 12\frac{1}{4}^\circ$; whereas, with bleed it dropped from 85.8 to 79.5 percent over the same range of α.

The effect of bleed on center body 1 at $\theta_l = 40.0^\circ$ was to improve the maximum pressure recovery at angles of attack above 4° with approximately equal performance at lower values of α. At an angle of attack of 0° both with and without bleed, center body 1 at $\theta_l = 40.0^\circ$ had a

maximum pressure recovery of 87.4 percent. The pressure recovery without bleed dropped to 77.8 percent at $\alpha = 12\frac{1}{4}^{\circ}$; whereas, with bleed it dropped to only 82.9 percent. Thus, configuration 1-40.0-S0 sustained a variation in maximum pressure recovery of only 4.5 percent over a $12\frac{1}{4}^{\circ}$ range in angle of attack.

The shadowgraphs in figures 8 and 9 of the minimum stable flow of the various configurations of center body 1 at $\alpha = 0^{\circ}$ to $12\frac{1}{4}^{\circ}$ provide further information with which to assess the effectiveness of the boundary-layer bleed. Bleed is ineffective in alleviating the vortex type of instability occurring when the conical shock strikes the cowling lip at critical mass flow (figs. 8(a) and 8(e)). However, when either all or part of the conical shock is ahead of the lip as a result of angle of attack (fig. 8 for $\alpha > 0^{\circ}$) or positioning of the cone ahead of the design location (fig. 9) so that mass-flow spillage may be accomplished with part of the vortex outside the cowling, bleed is effective because it retards the separation which occurs after the shock and which results in instability for these conditions. The limiting stable position with complete circumferential boundary-layer bleed on center body 1 then is determined by either the vortex sheet intersecting the cowling lip (figs. 8(f), 8(g), and 9(e)) or the normal shock reaching the flush slots (figs. 8(h), 9(f), 9(g), and 9(h)). The vortex-type limitation under such conditions was first noted and discussed in reference 3. The flush-slot limitation appears logical, especially at values of $\alpha > 0^{\circ}$ since the passage of the upper shock across the slot would create a pressure differential between the top and bottom halves of the slot which would retard or even reverse the boundary-layer removal from the lower surface and thereby promote separation.

The Mach number contours of figure 10, although drawn for inlet 1-40.0-S0 at $\alpha = 8^{\circ}$, are also representative of the other stability conditions of shock at slot for this center body and are indicative of separation further forward in the inlet as the mass flow is reduced from critical to minimum stable values. These contours indicate that the separation behind the upper-surface shock may also be a contributing factor to instability in this case, although the relative position of shock to slots logically appears to be the more important factor.

It should be noted that the above results regarding the effectiveness of bleed and the relative location of vortex sheet and cowling lip are applicable generally but not universally since conditions such as unusual values of θ_l/θ_s or subsonic diffusion rates, which are not usually associated with high performance inlets, may not agree with these results. Such a case of unusual diffusion rate is discussed in regard to center body 4 in a later section of this paper.

An investigation was also made of the effect of boundary-layer removal on either the upper or lower surface of the cone at values of $\alpha = 4^\circ$ and 8°. The stable subcritical ranges of center body 1 at $\theta_l = 42.5^\circ$ with bottom slots open and top slots open were the same as the ranges obtained when the bleed slot was completely closed or open, respectively. However, for center body 1 at $\theta_l = 40^\circ$, although the stable range with bottom slot open was again the same as the no-bleed condition, the use of bleed on only the upper surface of the center body permitted a stable mass-flow reduction roughly half that obtained when full bleed was used. (See fig. 7(a).)

The explanation for the effectiveness of only the top slots in relation to the effectiveness of the complete slots may be found in the following observations: A comparison of figure 11(a) with figure 11(e) and figure 11(c) with figure 11(g) reveals that, at minimum stable flow with top slots open, the distance from the foot of the top so-called normal shock to the slot is approximately the same at the same angle of attack for both $\theta_l = 42.5^\circ$ and 40°. In other words, at a given α the upper slot section can deter the boundary-layer crossflow to such an extent that the shock may advance to a certain distance behind the slots before the crossflow boundary layer flowing in behind it becomes large enough to cause separation. The normal shocks ahead of the cowling on the sides of the central body are thickening the crossflow boundary layer which passes through them. The separation causing instability arises from a combination of this thicker crossflow boundary layer undergoing some external compression and then accumulating on the upper surfaces of the central body in a region of adverse pressure gradient inside the cowling. For $\alpha = 4^\circ$ and 8°, the distance from the shock to the slots at minimum stable flow with only top slots open is apparently less than, or coincides with, that distance at which instability arises because the vortex sheet strikes the lip when $\theta_l = 42.5^\circ$ (see figs. 8(f), 8(g), 11(a), and 11(c)) so that the same stable subcritical range is obtained with full slots and only top slots in this case. However, for $\theta_l = 40^\circ$ this distance for top slots open is more than the zero distance (shock at slot) when full slots are used so that the range is correspondingly smaller (see figs. 9(f), 9(g), 11(e), and 11(g)).

The complete lack of effectiveness of the bottom slots at $\alpha > 0^\circ$ was expected since slots in such a location can do little to prevent the boundary-layer crossflow from bottom to top of the cone ahead of the shock; consequently, the boundary layer in the vicinity of the upper shock has been only slightly reduced, if at all.

Tests at an angle of attack of 0° were also run of the inlet configuration combining center body 4 with cowling B. Inspection of figure 5 shows that this cowling and center-body combination had a very poor distribution of area with axial distance; the rate of subsonic diffusion in the first 1/2 hydraulic diameter was equivalent to a

conical diffuser with an included angle of 20° or more. As expected, center body 4 with cowling B had poorer pressure recovery than center body 1 with cowling A (see fig. 7(b) because of the inefficient subsonic diffusion. However, an unexpected result was that the stable mass-flow range of center body 4 for $\theta_l = 42.4°$ (shock on lip) was increased to 6.5 percent for both no-bleed and flush-slot control and up to 10 percent by the use of the scoop slot. Since both slots capture the computed boundary layer, the variation between the scoop- and flush-slot performance might be explained by the fact that the shock patterns near the cowling lip are not identical, because, in the case of the scoop inlet, the oblique shock from the scoop intersects the conical shock in the region of the lip. Consequently, the conical-shock position is between that which it would occupy for flow about a cone with retracted tip (scoop inlet) or extended tip (flush inlet) when this shock intersects the normal shock (see fig. 12).

No reason is known for the unexpected conical shock-on-lip stable subcritical range for the no-bleed and flush-slot configurations unless the very rapid area increase, which is usually associated with a destabilizing influence, is such that separation occurs inside the cowling even in critical flow so that the effective flow area and adverse pressure gradient are reduced markedly. Under these conditions, a vortex sheet could enter and mixing could occur before diffusion. However, it should be noted that combustion-chamber Mach number profiles indicate that, if any unusual separation for either critical or minimum stable flows exists inside the cowling, reattachment occurs upstream of the rake.

Center body 4 at $\theta_l = 39.5°$ had a higher stable mass-flow range than center body 1 at $\theta_l = 40°$, with no boundary-layer bleed, but both flush and scoop boundary-layer bleeds were much less effective on center body 4 than the flush bleed on center body 1. (See fig. 7(a).) The limiting stable condition was largely influenced by the curvature of center body 4; the curvature at the entrance when $\theta_l = 39.5°$ promoted separation after the shock and thereby initiated buzzing (figs. 12(d), 12(e), and 12(f)).

Performance comparison of conical center body employing boundary-layer bleed with pivoted-cone and "constant area" throat inlets.- A comparison of the performance of center body 1 employing bleed as a method of controlling buzz with that of 25° semicone-angle conical diffusers using a pivoted cone and essentially constant-area throat (refs. 4 and 6) is presented in figure 13. The data of figure 13 for these particular diffusers are cross plots of the figures in the above references. The performance of the pivoted-cone inlet (which had a low rate of diffusion of only 1.5 percent per hydraulic diameter for the initial 3 hydraulic diameters) for $M = 1.91$ and $\theta_l = 41.8°$ (2.2° less than the shock angle of 44°) is compared with that of center body 1 at

$\theta_l = 40^\circ$ (2.4° less than the shock angle of 42.4°) at $M = 2.02$. The stable mass-flow range of center body 1 with bleed is greater than that for the pivoted cone for all angles of attack investigated. It might be noted that tests results reported in reference 6 for the pivoted cone with the conical shock slightly inside the cowling lip ($\theta_l = 44.7^\circ$) showed stable ranges appreciably greater than those mentioned herein. However, the vortex for this configuration was inside the cowling at supercritical conditions (thus, the instability caused by the vortex on the lip was probably eliminated), and no comparable tests were conducted on center body 1. The rate of decrease in maximum pressure recovery with angle of attack is approximately the same for center body 1 and the pivoted cone with axis of the cone alined with the free stream. Furthermore, the effect on maximum p_o of pivoting the cone and using bleed is roughly the same at the higher angles of attack. The shaded area of figure 13 indicates the increase of maximum p_o due to bleed and cone pivoting.

The stable mass-flow range for configuration 1-40.0-SO is also compared with that of a 25° conical inlet having "zero" subsonic diffusion (1 percent area-ratio variation per hydraulic diameter for 3.5 hydraulic diameters) with $\theta_l = \theta_s$ at $M = 2.0$. The stable range of the zero-diffusion-rate inlet exceeds that of center body 1 for angles of attack below 4°, after which the opposite result is noted. This trend is due to the large decrease in the stable range of the zero-diffusion-rate inlet at $\alpha = 3.5^\circ$, whereas center body 1 with bleed has a nearly constant range. No applicable pressure-recovery data were given for this model in reference 4.

On the basis of these results (at conditions in which $\theta_l \leqq \theta_s \leqq \theta_l + 2.4^\circ$), the use of boundary-layer bleed on a conical center body compares favorably with the use of a pivoted cone and constant-area diffusion as a method of increasing the stable subcritical performance. Of course, bleed could also be incorporated with the other methods to optimize performance.

Fluted-body boundary-layer control.- Results of tests performed upon eight-fluted center body 2, with and without boundary-layer bleed, are presented in figure 14, in which the variations of stable subcritical mass-flow range and minimum stable pressure recovery with angle of attack are summarized.

The tests of fluted center body 2 with an effective cone angle of 24.7° may be used to assess the value of such vortex generation by comparison of the test results (fig. 14) with those of center body 1 (fig. 7). The stable mass-flow range of inlets 2-42.4-SC and 2-39.7-SC is approximately the same as that of inlets 1-42.5-SC and 1-40.0-SC. However, boundary-layer bleed has no beneficial effect either on the

stable subcritical range of center body 2 or on the maximum pressure recovery which in general decreases with angle of attack. At $\alpha > 0^{\circ}$, buzzing appeared to be due to separation at the foot of the λ-shock on the upper surface since local oscillations appeared in that region before the whole shock system began to oscillate. Figures 15(a), 15(b), and 15(c) are shadowgraphs showing minimum stable flows for center body 2. The tests of this center body result in the following conclusion: The use of flutes on a center body to act as vortex generators at $\alpha > 0^{\circ}$ or to inhibit cross flow has no advantages without boundary-layer bleed and, moreover, is disadvantageous with boundary-layer bleed when compared with an unfluted body of equivalent cone angle.

Effect on Stable Range of Distortion of Conical Shock

Inasmuch as the entrance into the cowling of the vortex sheet from the intersection of the conical and normal shocks is one of the causes of instability, experiments were run to see whether distortion of the conical shock, and consequently of this vortex sheet, could permit an increased stable range by allowing gradual introduction of the vortex. Center body 3 was designed for this purpose and shadowgraphs, which were taken of the center body alone in the air stream with both the plane of a flute and then the plane of a valley perpendicular to the light beam, showed a radial distortion of the conical shock. This distortion, measured at the location of the cowling lip, was 0.06 inch, or six times the thickness, of the cowling lip. Test results showed not only a lack of any significant stable subcritical range at any angle of attack but also very poor pressure-recovery characteristics (fig. 14(b)). The latter result was expected since, in order to obtain conical shock distortion at the cowling, extreme deformation of the center body is required, and the flow over such a center body probably contains many undesirable boundary-layer characteristics. The buzzing appeared to originate at the foot of the λ-shock on the top ridge of the center body, and this, rather than the vortex sheet, was the determining factor (see fig. 16) for most configurations. For center body 3 at $\theta_l = 47.9^{\circ}$, the vortex sheet may have been the cause of instability in some cases because there was no evidence of a prominent λ-shock (figs. 16(a) and 16(c)). These tests then indicate that distortion of the vortex sheet in this manner and degree (six cowling-lip thicknesses) is impotent as a stabilizing device. The ineffectiveness of distortion of the shock as found in this case should not be construed to rule out application of the idea to all inlets; reference 7 reports some beneficial effects for the use of a vertical wedge-type center body in a modified cowling.

It might be noted at this point, although the data are not shown, that the effect of fairing and rounding off the flutes (fig. 4) had no effect on the stable range and a small effect on maximum pressure

recovery. This small effect increased the pressure recovery about 1 percent for center body 3 and caused increases and decreases of about 0.5 percent for center body 2 at $\theta_l = 42.4^\circ$ and 39.7°, respectively.

Effect on Stable Range of Cowling-Lip Thickness

The effect of cowling-lip thickness was investigated at an angle of attack of 0° with center body 1 and cowling A. Tests were conducted with the cowling-lip thickness increased from the normal value of 0.010 inch (used in the other tests) to 0.040 inch and decreased to 0.003 inch by varying the outer contour, the inner surface remaining unchanged. The results of the tests are summarized in figure 17, and shadowgraphs of the minimum stable flows are shown in figure 18.

For $\theta_l = 42.5^\circ$, the lip thickness had no significant effect on the stable range, which was negligible for both slots open and closed, but it did result in maximum p_o decreasing as lip thickness was increased.

For $\theta_l = 40^\circ$ with no bleed, however, increasing the cowling-lip thickness increased the stable mass-flow range from 3 percent when the cowling-lip thickness was 0.003 inch to 6.5 percent when the cowling-lip thickness was 0.040 inch (fig. 17(a)). The shock positions at minimum stable mass flow are shown in figures 18(d), 18(e), and 18(f). It should be mentioned that the apparent front legs of a λ-shock in figure 18(d) are due to weak waves arising from a slight disturbance in the fairing closing the slots and are not due to separation.

The minimum stable mass flow for $\theta_l = 40.0^\circ$ was approximately the same (87.8 ± 0.6 percent m_o) for the three cowling-lip thicknesses without bleed, and the increase in stable range is a result of the critical mass flow increasing as the lip is thickened. An increase in maximum mass-flow spillage with an increase in lip thickness is evident from the shadowgraphs of figures 18(d), 18(e), and 18(f), which show the shock at the minimum stable-flow position to be farther ahead of the lip for the thicker lips than for the thinner lips. The increase in critical mass flow is due to the fact that the limiting streamline, separating the captured mass flow from that flowing around the inlet, has a stagnation point at some average radius between the outer and inner cowling radii; consequently, as the outer radius is increased while the inner radius remains constant, the radius to the stagnation point of the limiting streamline increases at supercritical conditions.

The instability was not caused by the vortex sheet for $\theta_l = 40^\circ$ and with slots closed but rather by separation to the rear of the shock on the center body or cowling inner surface. One possible favorable condition which led to the improved closed-slot stability might have

been a negative pressure gradient established in the vicinity of the inlet plane. This pressure gradient was caused by the contraction of the stream tube as the flow area decreased from that determined by the radius of the stagnation point of the limiting streamline to the area determined by the cowling inner radius.

For $\theta_l = 40^\circ$ and with boundary-layer bleed, thickening the cowling lip has the effect of first increasing slightly and then markedly decreasing the stable subcritical range (fig. 17). The values of minimum stable mass flows were 0.744, 0.753, and 0.857 for lip thicknesses of 0.003, 0.010, and 0.040 inch, respectively. The cause of buzz appeared to be the vortex sheet impinging on the cowling lip (figs. 18(g), 18(h), and 18(i)). Inasmuch as the vortex sheet cannot have a steady stagnation point on the cowling lip because of the different total pressures across the sheet, and since the vortex would first contact the cowling with the larger outer radius, it is logical that the unstable pattern should occur at a higher value of mass flow for the thicker cowling lips.

The behavior of the inlet at an angle of attack of 0° for $\theta_l = 40.0^\circ$ with and without bleed as the lip thickness is varied may be summarized as follows: For the case without bleed, separation occurring after the shock is the cause of the instability. This separation effect may be alleviated, with a resultant increase in stable mass-flow range, either by establishing a negative pressure gradient with a thicker cowling lip or by using boundary-layer bleed. The latter method appears more effective than the former because it permits a stable flow range down to the condition where the vortex sheet strikes the cowling lip. If the two methods were combined, however, thickening of the lip would generally decrease the stable range; not only is the necessity of the favorable pressure gradient removed by the use of bleed but also the thicker lip with a cowling of larger outer radius would result in the vortex sheet intersecting the cowling lip at a higher value of mass flow (lower stable flow range). Thus, the effectiveness of bleed for $\theta_l = 40^\circ$ decreases as the lip thickness increases until there is only a 2-percent difference between the stable ranges with or without bleed for a cowling-lip thickness of 0.040 inch (fig. 17). Thickening of the cowling lip at $\theta_l = 40^\circ$ has only a very slight detrimental effect (less than 1 percent) on maximum pressure recovery (fig. 17(b)).

SUMMARY OF RESULTS

Tests of several modifications of the center body and cowling of a supersonic inlet at a Mach number of 2.02 and angles of attack up to $12\frac{1}{4}^\circ$ yield the following results:

1. For a conical center body with a subsonic diffusion rate roughly equivalent to that of a 1° included-angle conical diffuser and with cowling-position angle equal to the conical-shock angle, use of boundary-layer bleed resulted in an increase with angle of attack of the stable subcritical mass-flow range (which was negligible without bleed). The stable-flow range reached a maximum value of 8 percent of the capture-area mass flow at an angle of attack of $12\frac{1}{4}^{\circ}$. At the same angle of attack, bleed increased the maximum pressure recovery about 7 percent to a value of 79.5 percent. For this cowling-position parameter and an angle of attack of 0° bleed had no beneficial effects.

2. With cowling-position parameter of 2.4° less than the conical-shock angle for the same cowling and center body, the use of boundary-layer bleed resulted in a stable range approximately 12 percent greater that that of the inlet with no bleed over the entire range of angle of attack tested and with a maximum stable range of 16 percent at an angle of attack of 0°. Pressure recovery was increased with bleed a maximum of 5 percent at an angle of attack of $12\frac{1}{4}^{\circ}$ so that, with bleed, the maximum pressure recovery decreased only from 87.4 percent at an angle of attack of 0° to 83 percent at an angle of attack of $12\frac{1}{4}^{\circ}$. The performance of this inlet with bleed compared favorably over a range of angle of attack with the performance reported in NACA RM E53I30 and NACA RM E53E26 of pivoted-cone and zero-diffusion-rate inlets.

3. At angles of attack of 4° and 8°, the use of bleed on only the upper surface of the 25° conical center body had the same effect as the use of bleed over the entire circumference for conditions of shock angle equal to cowling-position angle. When the cowling-position angle was 2.4° less than the shock angle, bleed on only the upper surface resulted in a stable subcritical range approximately half that obtained with complete bleed. Performance with bleed on only the bottom surface was the same as that found with no bleed.

4. For a conical center body with a subsonic diffusion rate equal to or greater than a 20° included-angle conical diffuser at an angle of attack of 0°, boundary-layer bleed increased the stable range for configurations having shock both on and ahead of cowling lip.

5. Use of an eight-fluted center body was ineffective at angle of attack as a method of increasing the stable subcritical performance by boundary-layer control.

6. Use of a four-fluted center body, which produced a conical shock distortion at the cowling of six cowling-lip thicknesses, was ineffective as a method of increasing the stable subcritical performance by vortex-sheet distortion.

7. For configurations having a conical center body at an angle of attack of 0°, the following trends were noted as the cowling lip was thickened from 0.003 to 0.040 inch:

(a) For conical shock on lip with and without bleed, the stable range was always negligible and the peak pressure recovery decreased.

(b) For shock ahead of lip and no bleed, the stable range was doubled while the pressure recovery decreased 0.3 percent.

(c) For shock ahead of lip and boundary-layer bleed, the stable range was halved and the pressure recovery decreased about 1 percent. The net result of bleed and thickening of the lip was an increase in stable range from 3 to 15 percent at a thickness of 0.003 inch, from 5 to 16 percent at 0.010 inch, and only from 6.4 to 8.2 percent at 0.040 inch.

Langley Aeronautical Laboratory,
National Advisory Committee for Aeronautics,
Langley Field, Va., March 11, 1955.

REFERENCES

1. Oswatitsch, Kl.: Pressure Recovery for Missiles With Reaction Propulsion at High Supersonic Speeds (The Efficiency of Shock Diffusers). NACA TM 1140, 1947.

2. Trimpi, Robert L.: A Theory for Stability and Buzz Pulsation Amplitude in Ram Jets and an Experimental Investigation Including Scale Effects. NACA RM L53G28, 1953.

3. Ferri, Antonio, and Nucci, Louis M.: The Origin of Aerodynamic Instability of Supersonic Inlets at Subcritical Conditions. NACA RM L50K30, 1951.

4. Nettles, J. C.: The Effect of Initial Rate of Subsonic Diffusion on the Stable Subcritical Mass-Flow Range of a Conical Shock Diffuser. NACA RM E53E26, 1953.

5. Obery, Leonard J., Englert, Gerald W., and Nussdorfer, Theodore J.: Pressure Recovery, Drag, and Subcritical Stability Characteristics of Conical Supersonic Diffusers With Boundary-Layer Removal. NACA RM E51H29, 1952.

6. Beheim, Milton A.: A Preliminary Investigation at Mach Number 1.91 of a Diffuser Employing a Pivoted Cone To Improve Operation at Angle of Attack. NACA RM E53I30, 1953.

7. Leissler, L. Abbott, and Hearth, Donald P.: Preliminary Investigation of Effect of Angle of Attack on Pressure Recovery and Stability Characteristics for a Vertical-Wedge-Nose Inlet at Mach Number of 1.90. NACA RM E52E14, 1952.

TABLE I

ORDINATES OF COWLING INNER SURFACES AND CENTER BODIES

Cowling				Center bodies									
A		B		1		2 (modified)			3 (modified)			4	
X	R	X	R	x	R	x	R_1	R_2	x	R_1	R_2	x	R
0	1.094	0	1.420	0	0	0	0	0	0	0	0	0	0
.30	1.162	.05	1.432	.323	.151	.088	.046	↑	.117	.117	↑	1.246	.583
.80	1.275	.10	1.443	.523	.268	.338	.178		.367	.366		1.327	.620
1.30	1.365	.15	1.455	.823	.385	.588	.308		.617	.540		1.407	.658
1.80	1.430	.20	1.466	1.073	.503	.838	.439	Linear variation	.867	.647		1.487	.694
2.30	1.485	.25	1.475	1.323	.620	1.088	.569		1.117	.727		1.568	.729
2.80	1.530	.30	1.483	1.573	.721	1.338	.693		1.367	.791		1.649	.758
3.30	1.560	.35	1.489	1.823	.809	1.588	.786		1.617	.846	Linear variation	1.689	.770
4.00	1.580	.40	1.495	2.073	.883	1.838	.870	.761	1.867	.888		1.729	.783
-----	↑	.45	1.500	2.323	.948	2.088	.939	.860	2.117	.950		1.769	.793
-----		.50	1.504	2.573	1.003	2.338	.994	.944	2.367	.957	↓	1.810	.799
-----		.55	1.507	2.823	1.051	2.588	1.042	1.021	2.617	.984	.953	1.850	.801
-----		.60	1.510	3.073	1.089	2.838	1.079	1.079	2.867	1.007	1.007	1.890	.802
-----		.65	1.513	3.323	1.121	3.088	1.111	1.111	3.117	1.027	1.027	1.971	.801
-----		.70	1.514	3.573	1.147	3.338	1.136	1.136	3.367	1.043	1.043	2.051	.800
-----		.75	1.516	3.823	1.168	3.588	1.156	1.156	3.617	1.055	1.055	2.253	.798
-----		.80	1.517	4.073	1.179	3.838	1.170	1.170	3.867	1.063	1.063	2.454	.795
-----		1.002	1.519	4.323	1.184	4.088	1.182	1.182	4.117	1.068	1.068	3.26	.786
-----		1.404	1.522	4.573	1.180	4.338	1.191	1.191	4.367	1.069	1.069	4.27	.775
-----		1.807	1.526	4.823	1.173	4.588	1.198	1.198	4.617	1.066	1.066	5.27	.763
-----		2.814	1.535	5.073	1.160	4.838	1.201	1.201	4.867	1.060	1.060	7.29	.740
-----		3.820	1.543	5.323	1.148	5.088	1.201	1.201	5.117	1.053	1.053	9.30	.717
-----		5.83	1.56	5.573	1.136	5.338	1.197	1.197	5.367	1.044	1.044	11.31	.694
-----		7.85	1.58	5.823	1.124	5.588	1.188	1.188	5.617	1.035	1.035	13.32	.671
-----	↓	9.86	1.67	6.073	1.111	5.838	1.176	1.176	5.867	1.025	1.025	15.10	.652
12.00	1.74	11.87	1.74	7.073	1.060	6.088	1.163	1.163	6.867	.985	.985	------	-----
12.5	1.76	12.50	1.76	8.073	1.008	7.088	1.105	1.105	7.867	.944	.944	------	-----
13.00	1.77	13.00	1.77	9.073	.956	8.088	1.047	1.047	8.867	.920	.920	------	-----
13.50	1.79	------	1.79	10.073	.904	9.088	.988	.988	9.867	.860	.860	------	-----
14.00	1.81	------	1.81	11.073	.851	10.088	.928	.928	10.867	.820	.820	------	-----
14.50	1.82	------	1.82	12.073	.799	11.088	.869	.869	11.867	.779	.779	------	-----
15.00	1.84	15.0	1.84	13.073	.748	12.088	.810	.810	12.867	.740	.740	------	-----
20.5	2.01	------	2.01	14.073	.696	13.088	.753	.753	13.867	.700	.700	------	-----
47.0	2.01	------	2.01	15.084	.642	14.088	.696	.696	14.872	.660	.660	------	-----
47.5	1.75	------	1.75	------	-----	15.093	.641	.641	------	-----	-----	------	-----
54.5	1.75	------	1.75	------	-----	------	-----	-----	------	-----	-----	------	-----

TABLE II

BOUNDARY-LAYER BLEED-SLOT DIMENSIONS

Center body	Slot leading-edge ordinate, x, in.	Slot trailing-edge ordinate, x, in.	Slot width, in.
1	0.900	0.972	-----
2	.900	1.100	0.125
3	.925	1.050	.250
4 (flush slot)	.900	.972	-----
4 (scoop slot)	.900	.927	-----

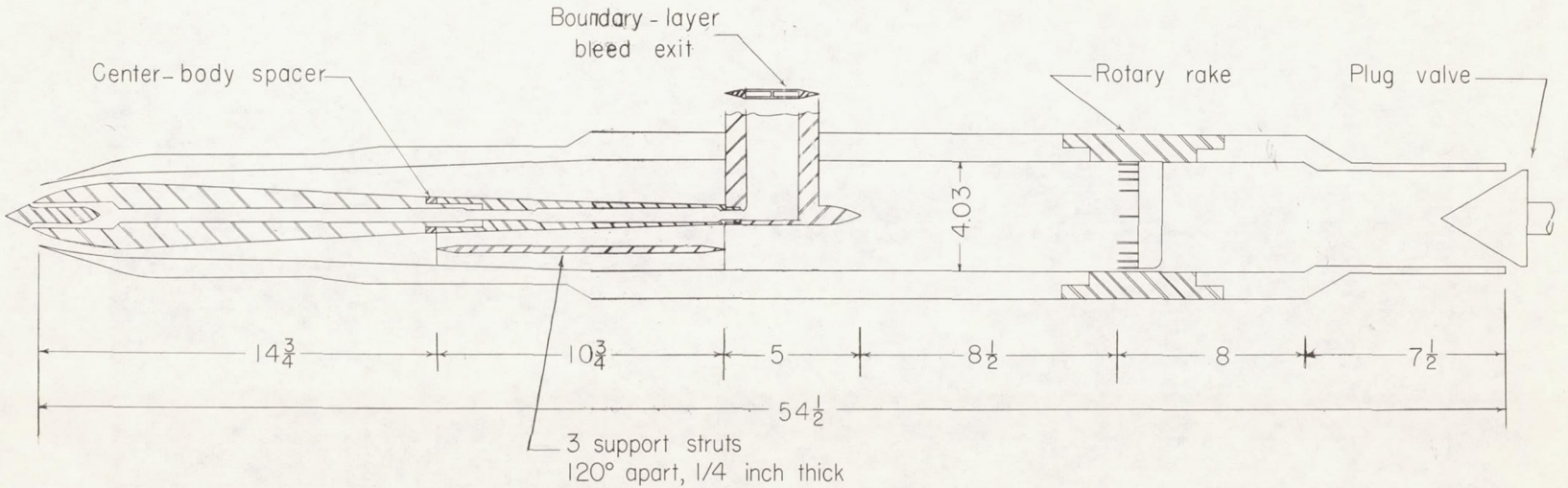


Figure 1.- Schematic diagram of model tested. Dimensions are in inches.

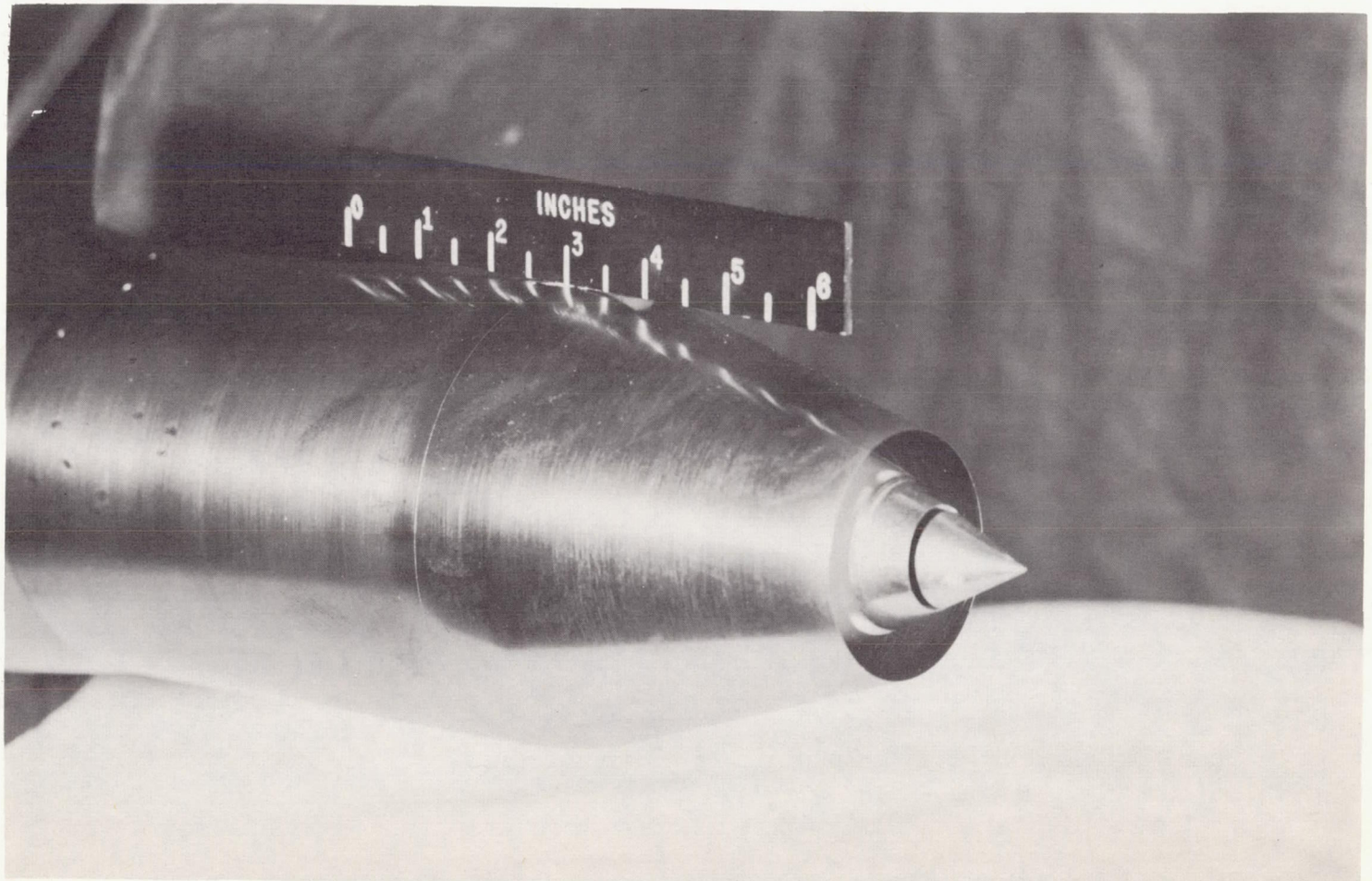


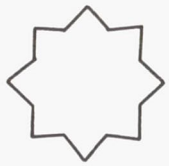
Figure 2.- Conical inlet. (Cowling A, center body 1.) L-87083



L-87081

Figure 3.- Center bodies 1, 2, and 3.

(a) Before transition.

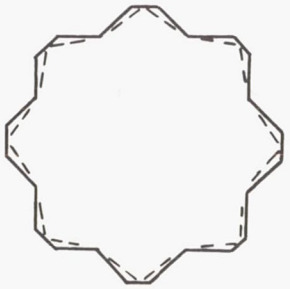


x = 0.8 inch



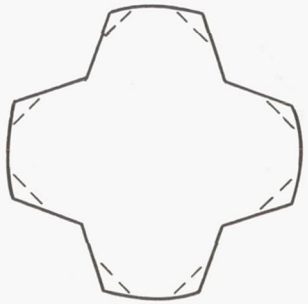
x = 0.3 inch

(b) During transition.



x = 1.6 inches

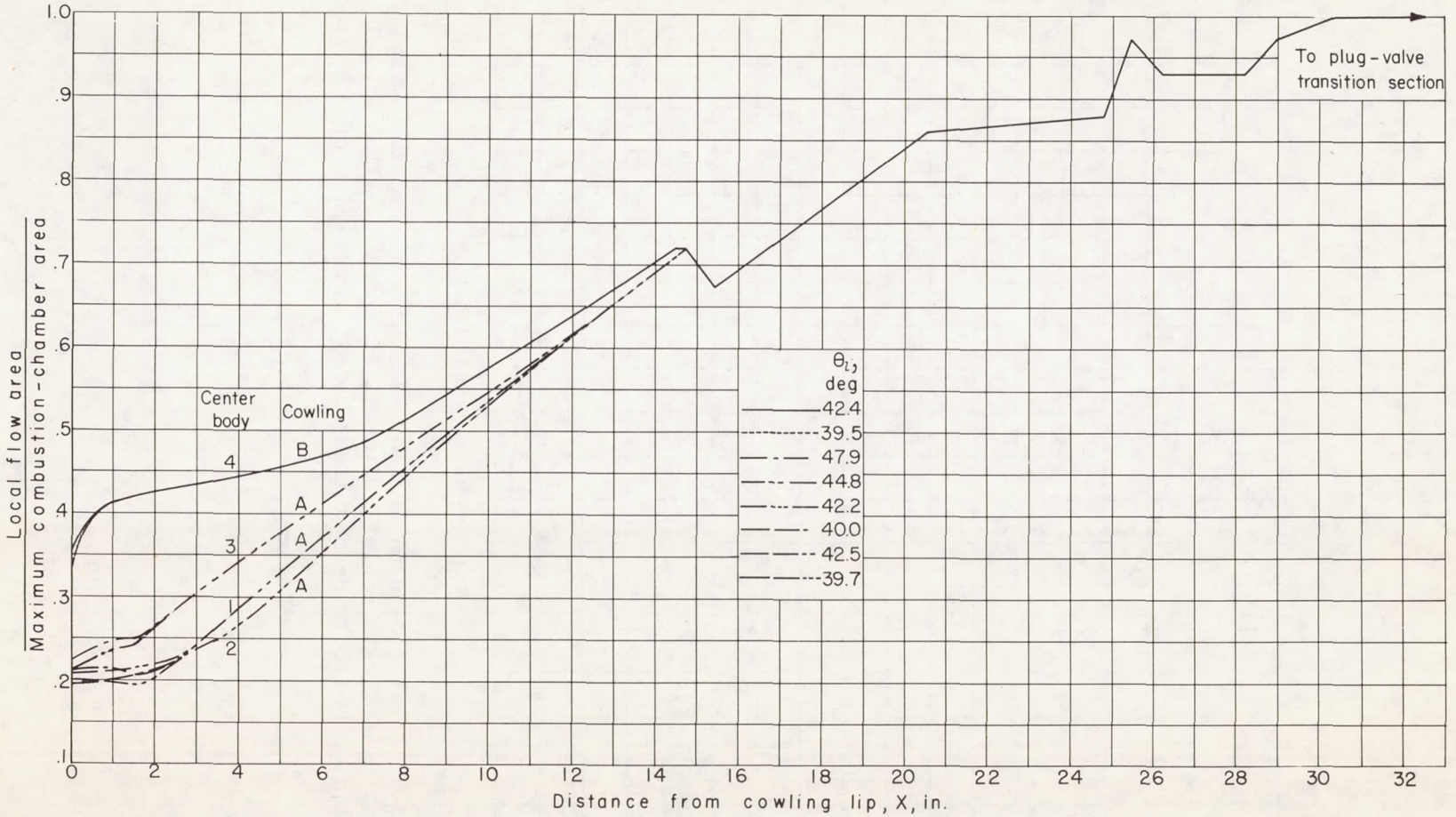
Center body 2



x = 1.6 inches

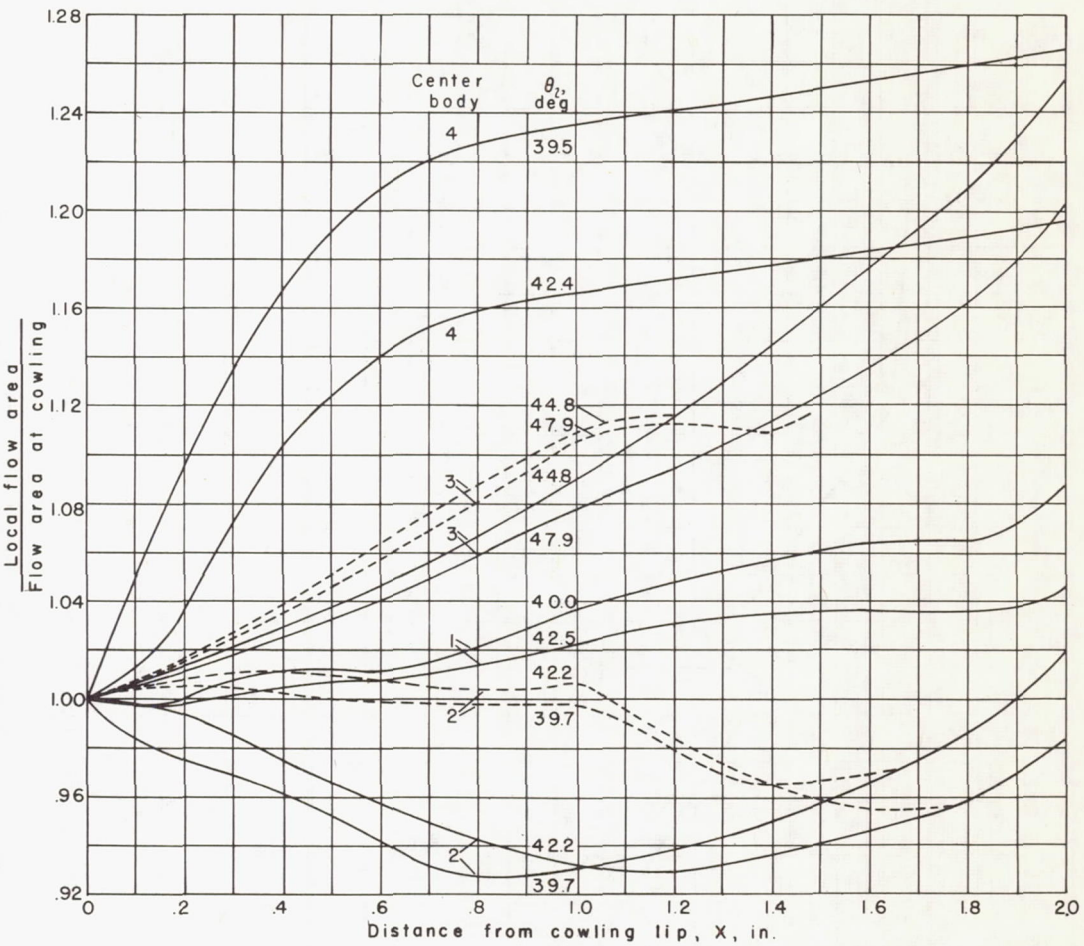
Center body 3

Figure 4.- Typical cross sections of center bodies 2 and 3. Dashed lines show modifications. x is distance from tip of center body.



(a) Ratio of local flow area to maximum combustion-chamber area.

Figure 5.- Area variations for various configurations.



(b) Ratio of local flow area to flow area at entrance to cowling. Cowling A used with center bodies 1, 2, and 3; cowling B used with center body 4. Dashed lines denote modified center bodies.

Figure 5.- Concluded.

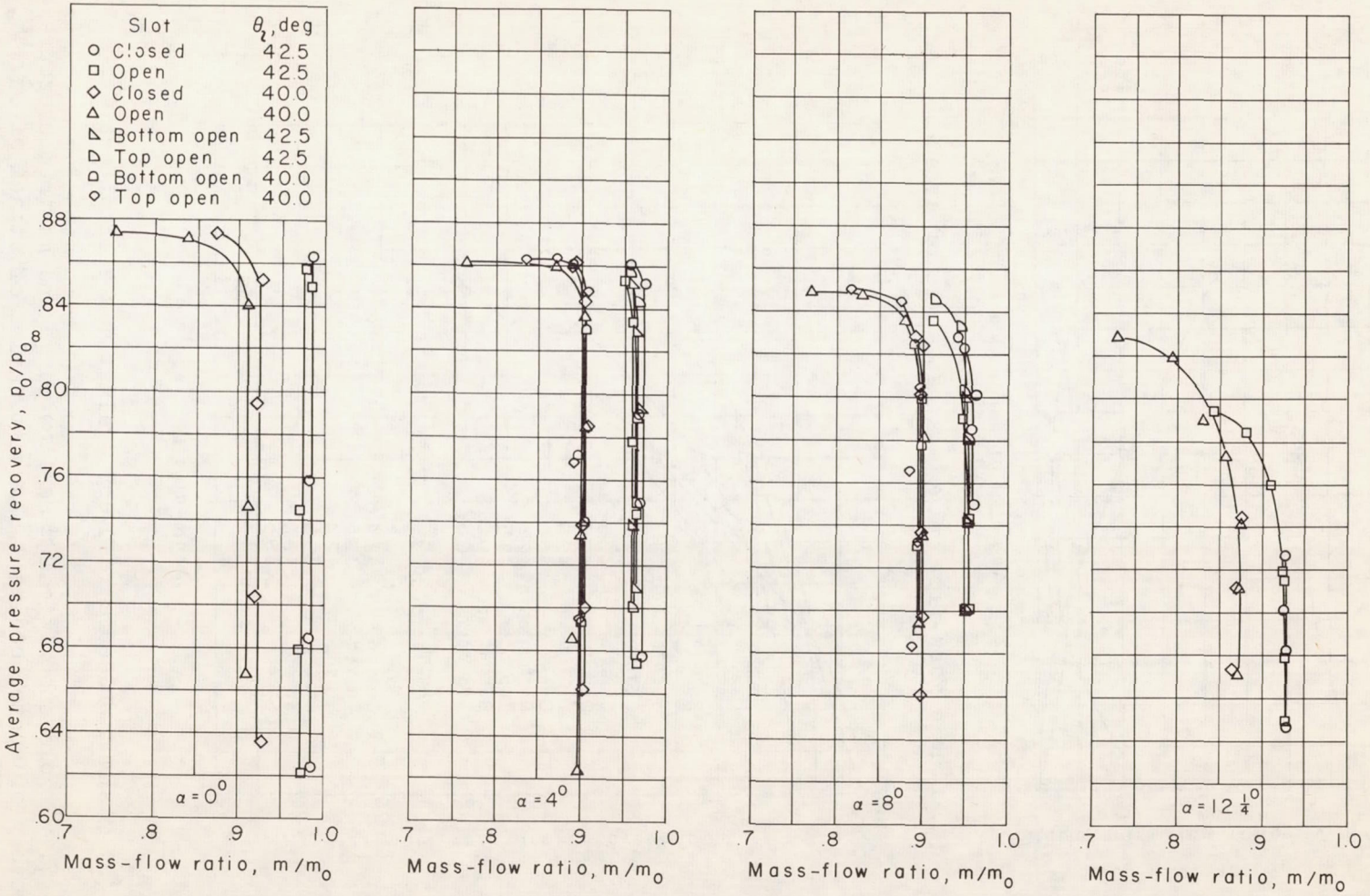
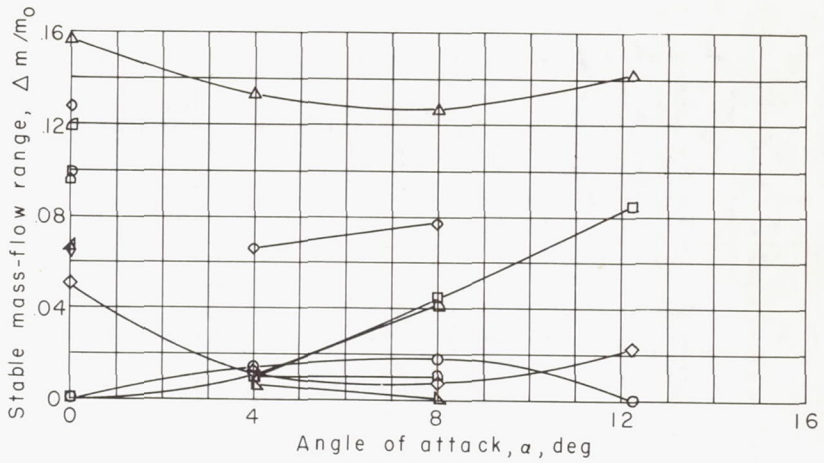
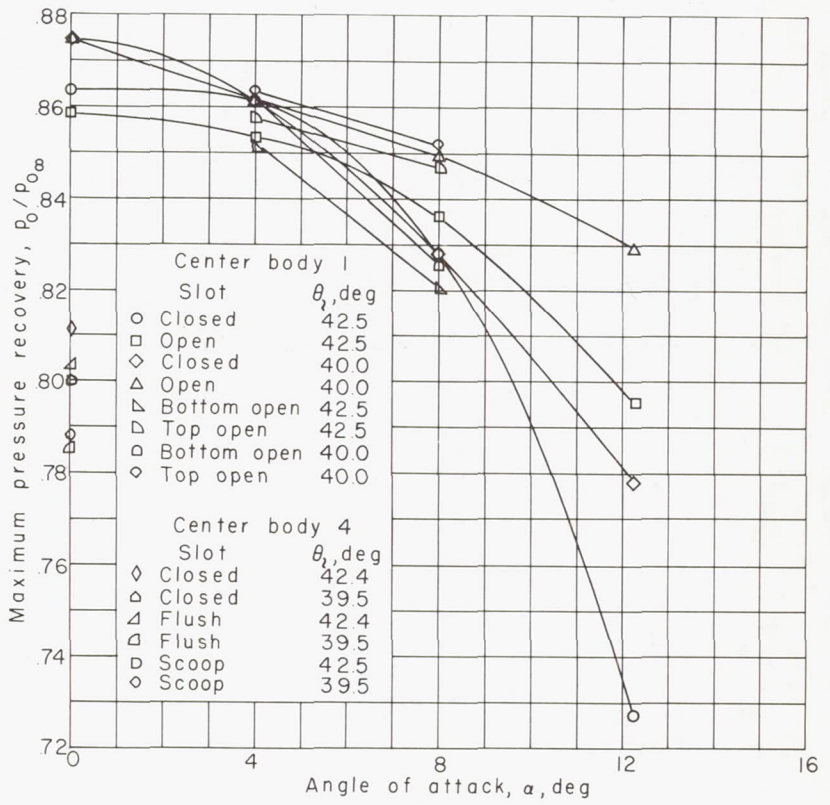


Figure 6.- Variation of average pressure recovery with mass flow for inlet employing center body 1 and cowling A at angles of attack of 0°, 4°, 8°, and $12\frac{1}{4}^\circ$.

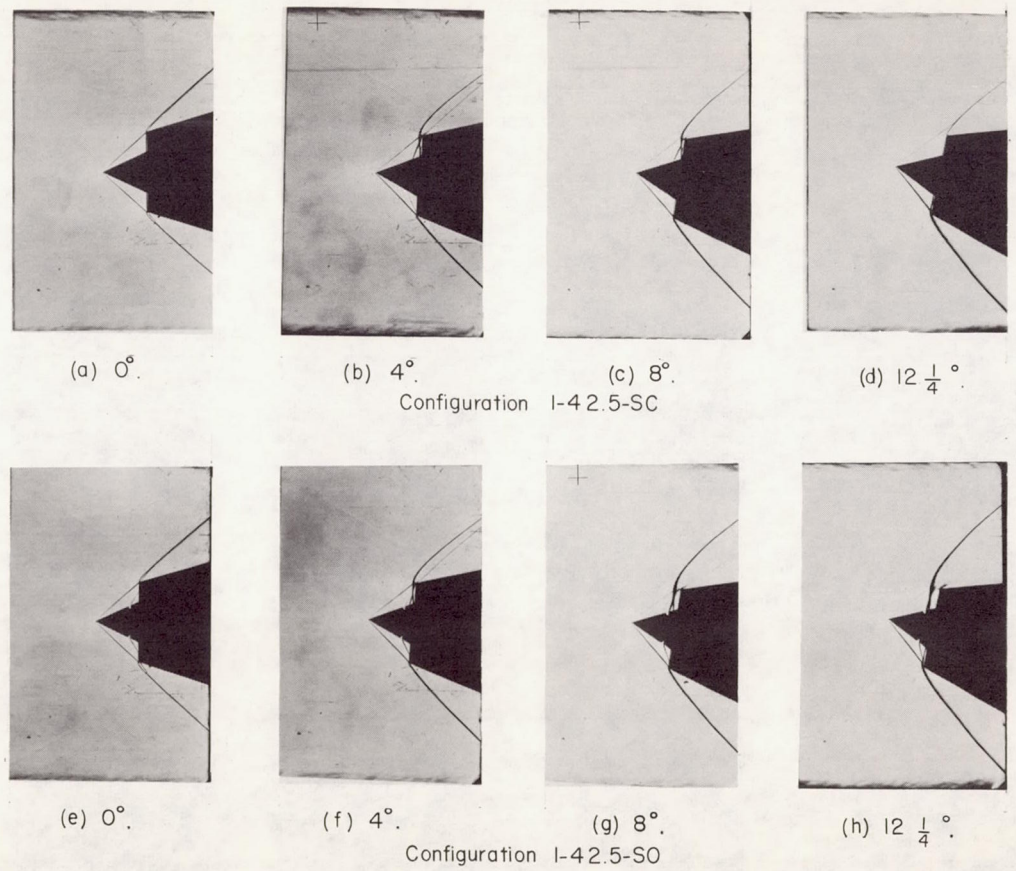


(a) Stable mass-flow range against angle of attack.



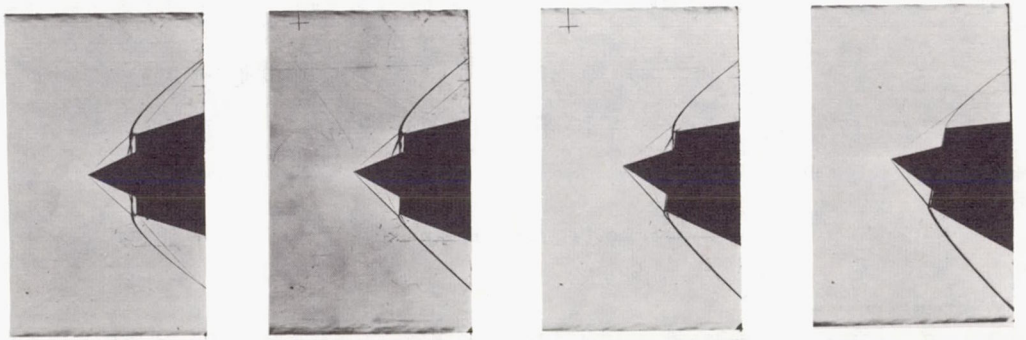
(b) Maximum pressure recovery against angle of attack.

Figure 7.- Stable subcritical mass-flow range and maximum pressure recovery of center bodies 1 and 4 at angles of attack of 0°, 4°, 8°, and $12\frac{1}{4}$°.



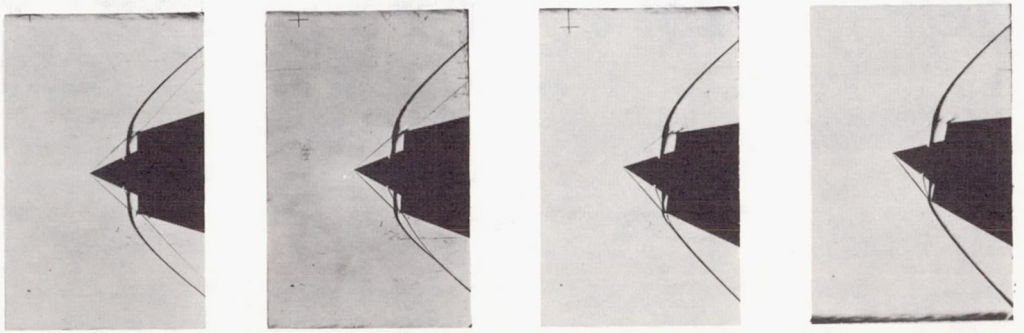
L-87912

Figure 8.- Shadowgraphs of minimum stable flow for configurations 1-42.5-SO and 1-42.5-SC at angles of attack of 0°, 4°, 8°, and $12\frac{1}{4}°$.



(a) 0°. (b) 4°. (c) 8°. (d) 12 $\frac{1}{4}$°.

Configuration 1-40.0-SC

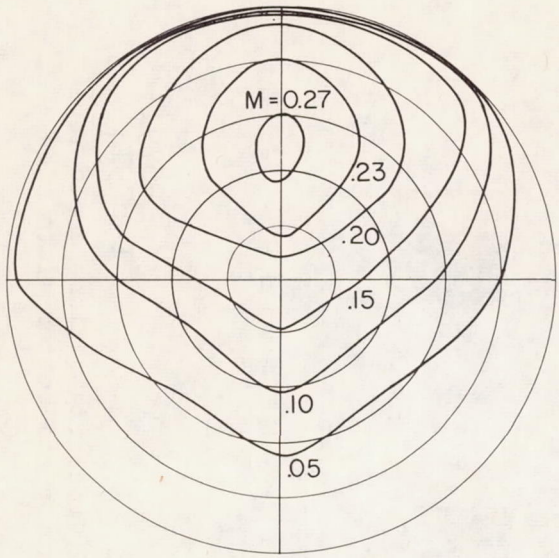


(e) 0°. (f) 4°. (g) 8°. (h) 12 $\frac{1}{4}$°.

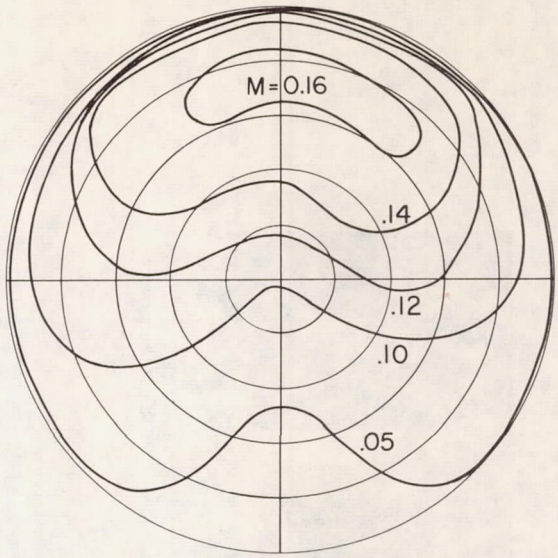
Configuration 1-40.0-SO

L-87913

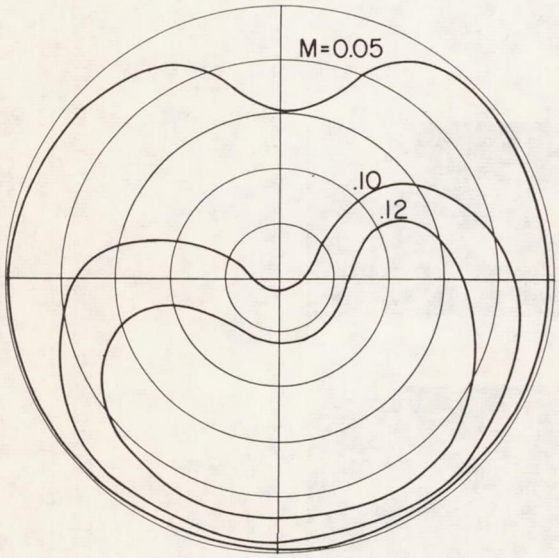
Figure 9.- Shadowgraphs of minimum stable flow for configurations 1-40.0-SC and 1-40.0-SO at angles of attack of 0°, 4°, 8°, and 12$\frac{1}{4}$°.



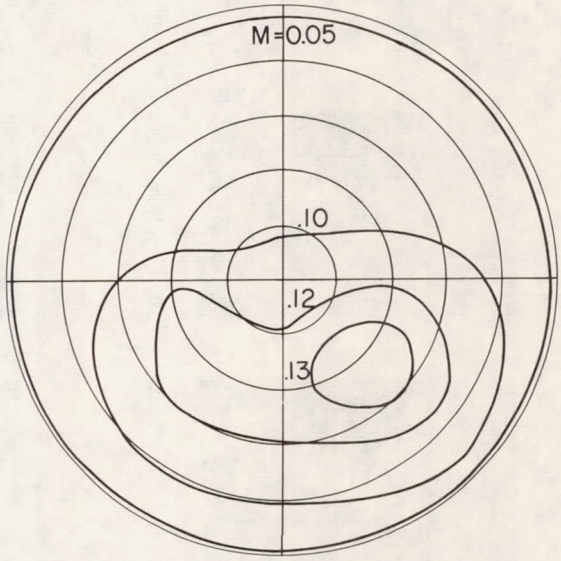
(a) Critical mass flow.
$m/m_0 = 0.899$; $p_0/p_{0\infty} = 0.809$.



(b) $m/m_0 = 0.881$; $p_0/p_{0\infty} = 0.835$.

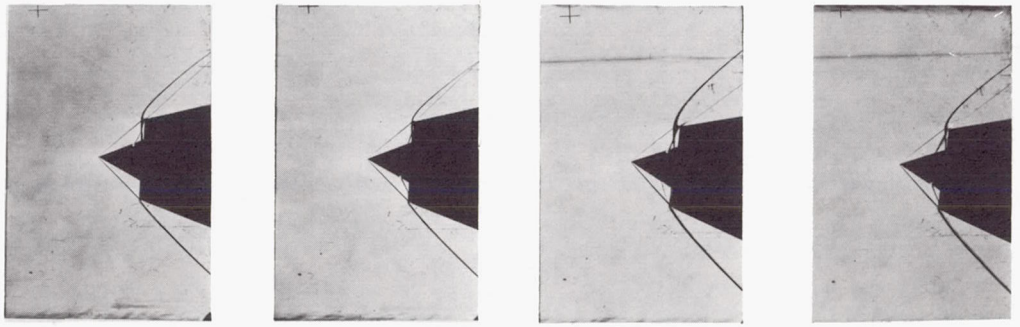


(c) $m/m_0 = 0.830$; $p_0/p_{0\infty} = 0.848$.



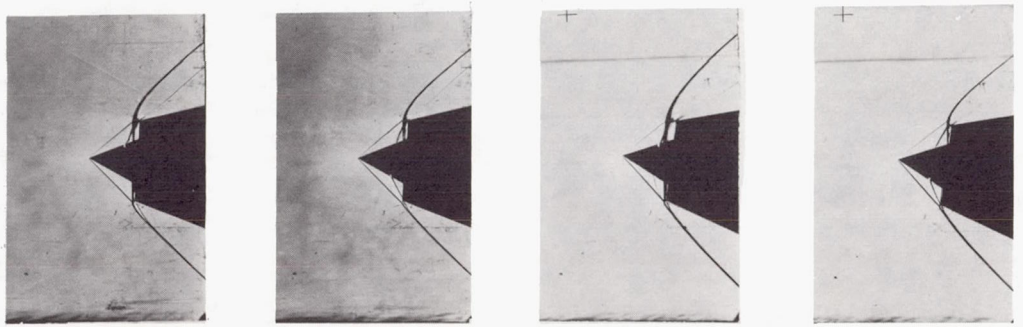
(d) Minimum stable flow.
$m/m_0 = 0.773$; $p_0/p_{0\infty} = 0.849$.

Figure 10.- Combustion-chamber Mach number contours for configuration 1-40.0-S0 at an angle of attack of 8°.



(a) 4°; top slots open. (b) 4°; bottom slots open. (c) 8°; top slots open. (d) 8°; bottom slots open.

θ_l = 42.5°

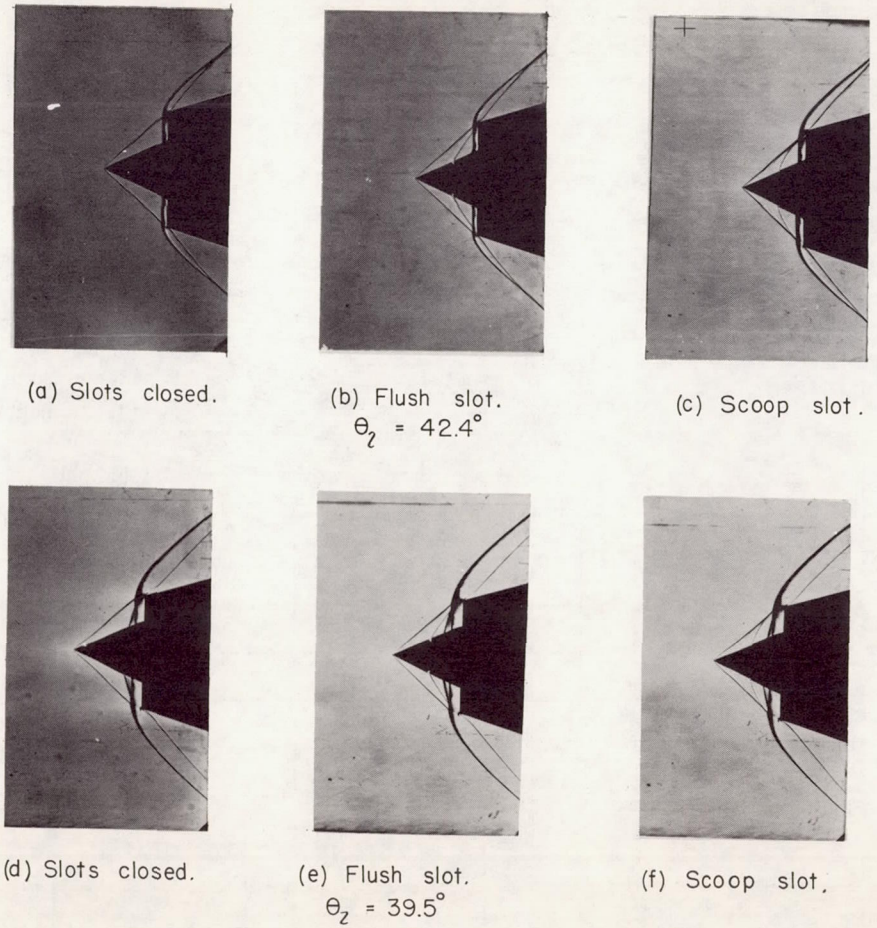


(e) 4°; top slots open. (f) 4°; bottom slots open. (g) 8°; top slots open. (h) 8°; bottom slots open.

θ_l = 40.0°

L-87914

Figure 11.- Shadowgraphs of minimum stable flow for configurations employing center body 1 and θ_l = 42.5° and 40.0° with top and bottom slots open at angles of attack of 4° and 8°.



(a) Slots closed.

(b) Flush slot. $\theta_l = 42.4°$

(c) Scoop slot.

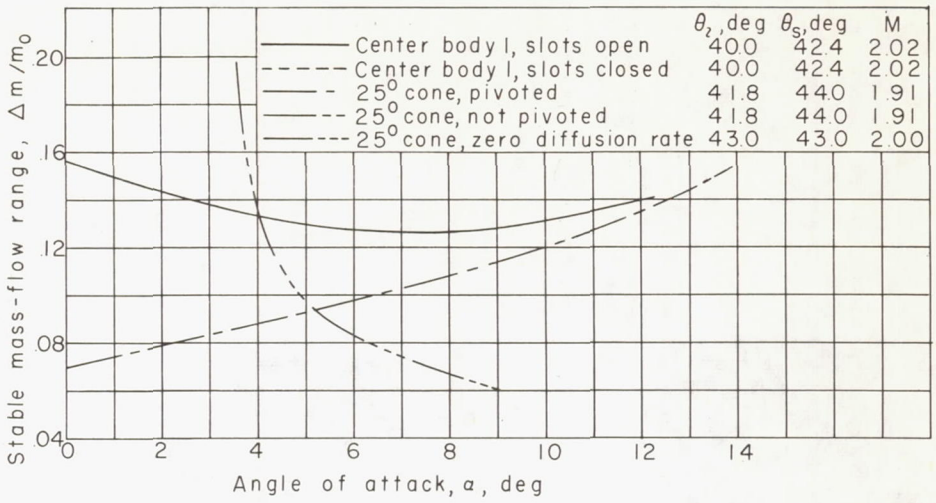
(d) Slots closed.

(e) Flush slot. $\theta_l = 39.5°$

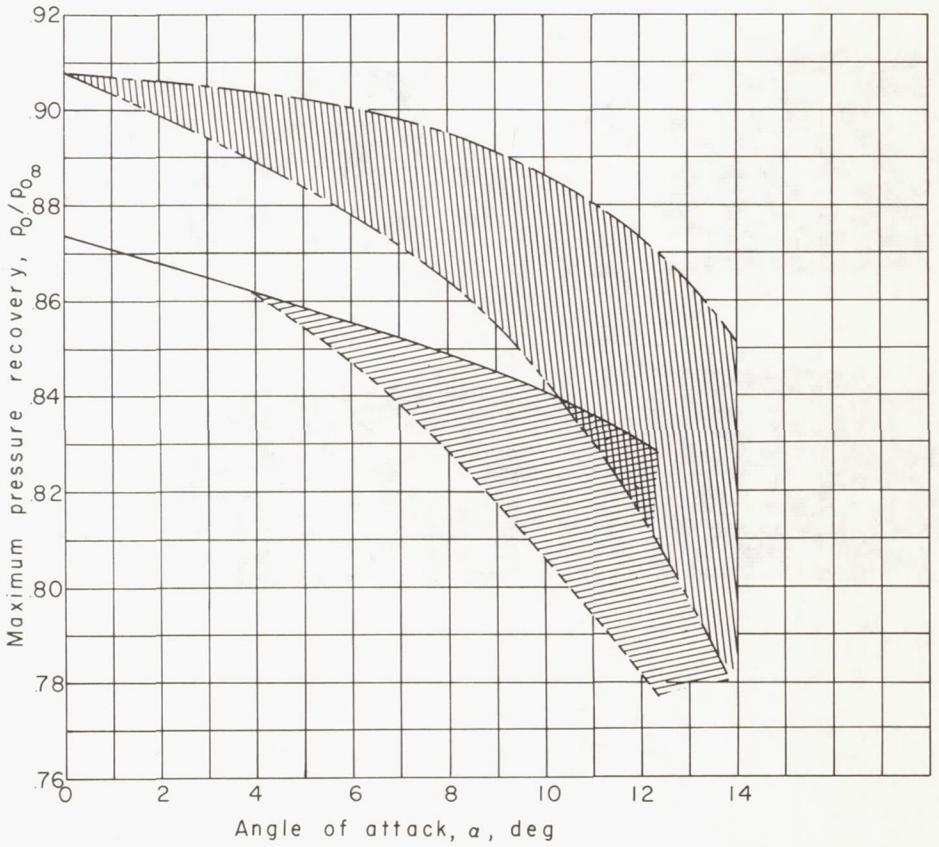
(f) Scoop slot.

L-87915

Figure 12.- Shadowgraphs of minimum stable flow for center body 4 and cowling B at an angle of attack of 0°.

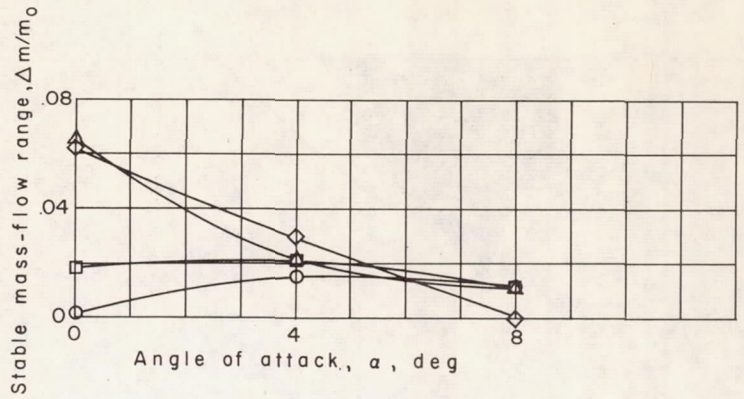


(a) Stable mass-flow range against angle of attack.

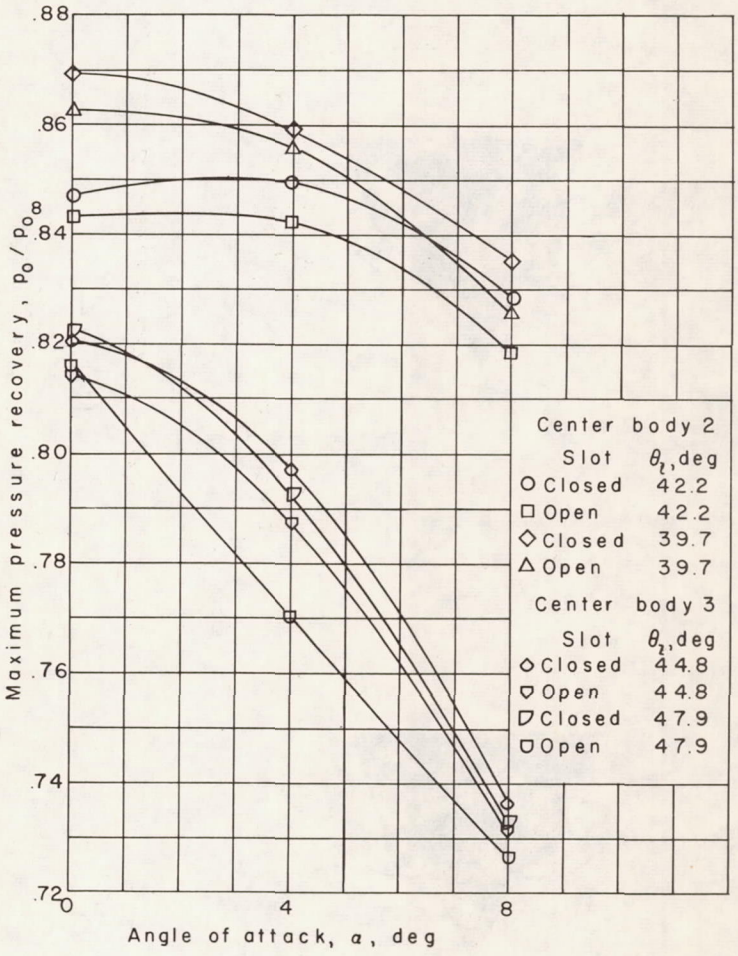


(b) Maximum pressure recovery against angle of attack.

Figure 13.- Comparison of performance of center body 1 with pivoted-cone and zero-diffusion-rate inlets.

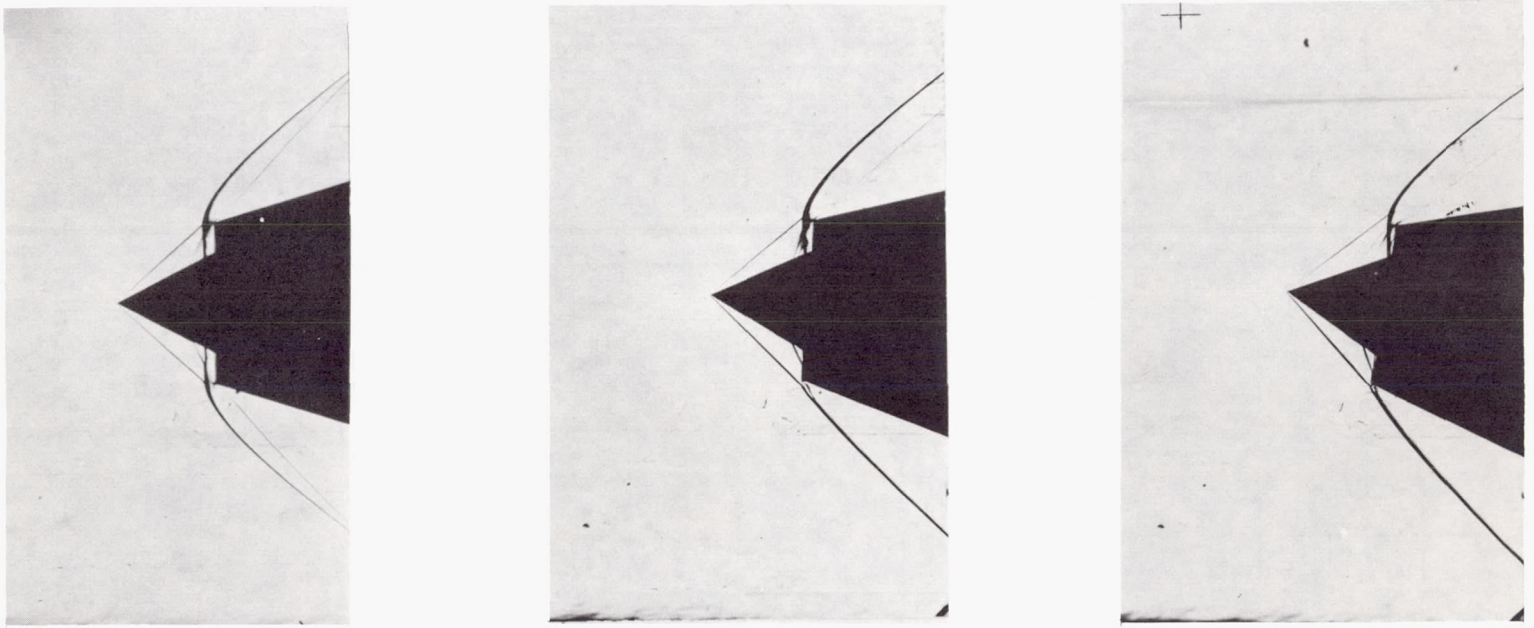


(a) Stable mass-flow range against angle of attack.



(b) Maximum pressure recovery against angle of attack.

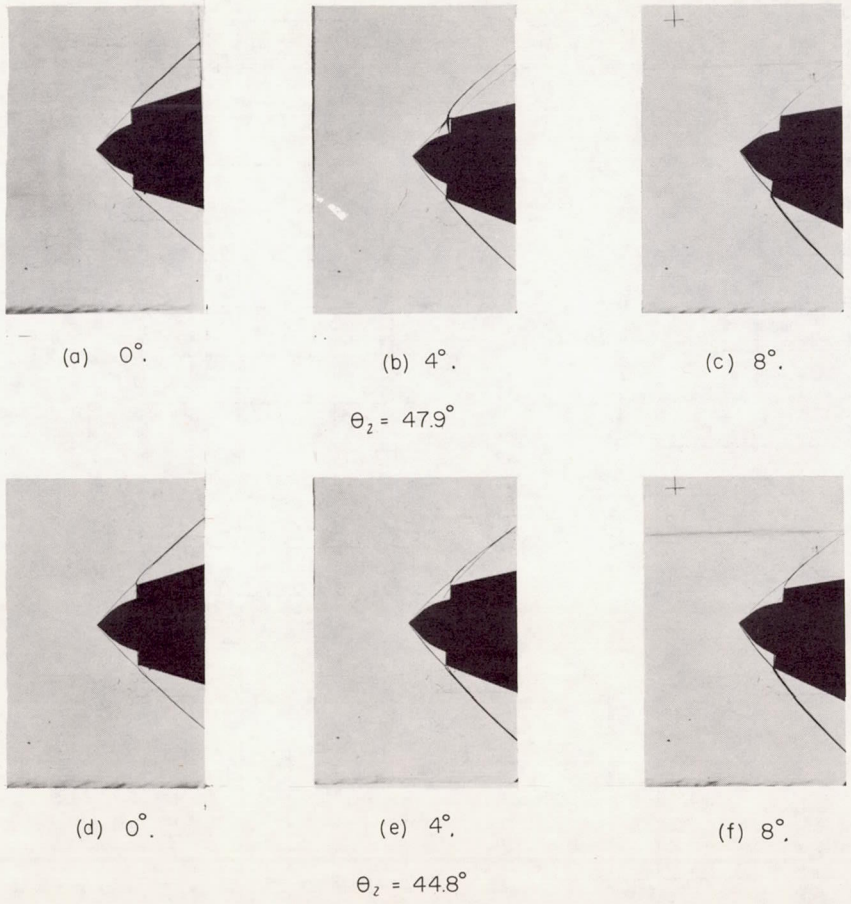
Figure 14.- Stable subcritical mass-flow range and maximum pressure recovery of center bodies 2 and 3 at angles of attack of 0°, 4°, and 8°.



(a) 0°. (b) 4°. (c) 8°.

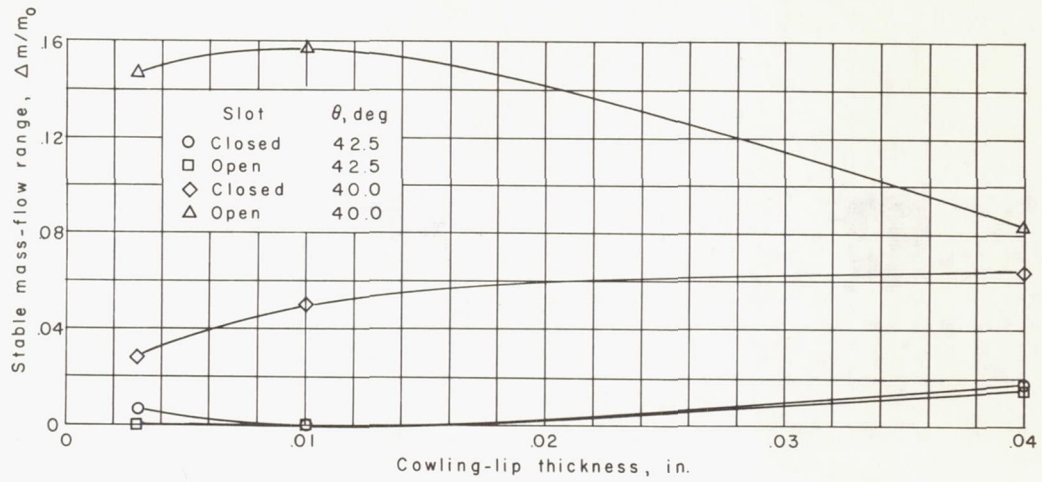
L-87916

Figure 15.- Shadowgraphs of minimum stable mass-flow pattern for configuration 2-39.7-S0 at angles of attack of 0°, 4°, and 8°.

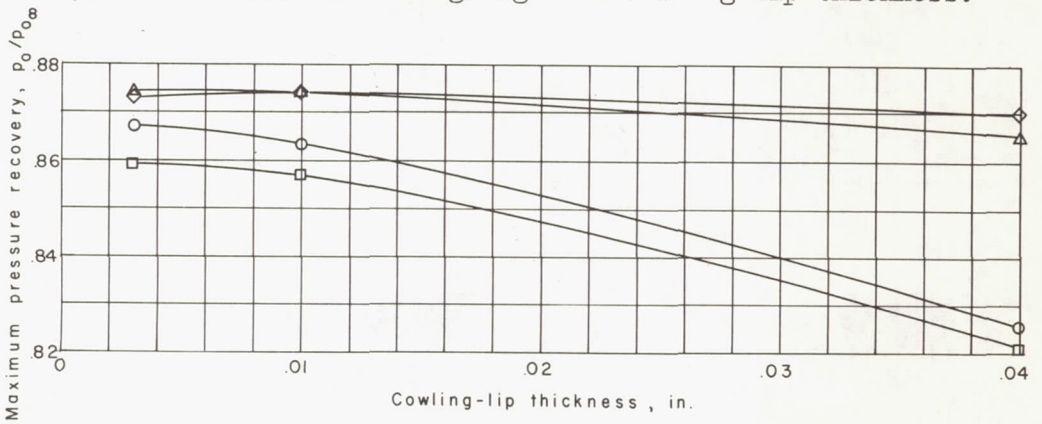


L-87917

Figure 16.- Shadowgraphs of minimum stable mass-flow pattern of configuration 3-47.9-S0 and 3-44.8-S0 at angles of attack of 0°, 4°, and 8°.

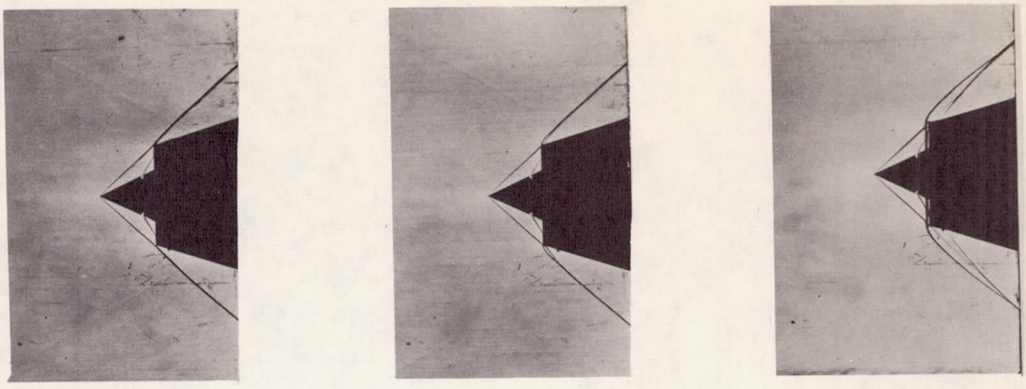


(a) Stable mass-flow range against cowling-lip thickness.

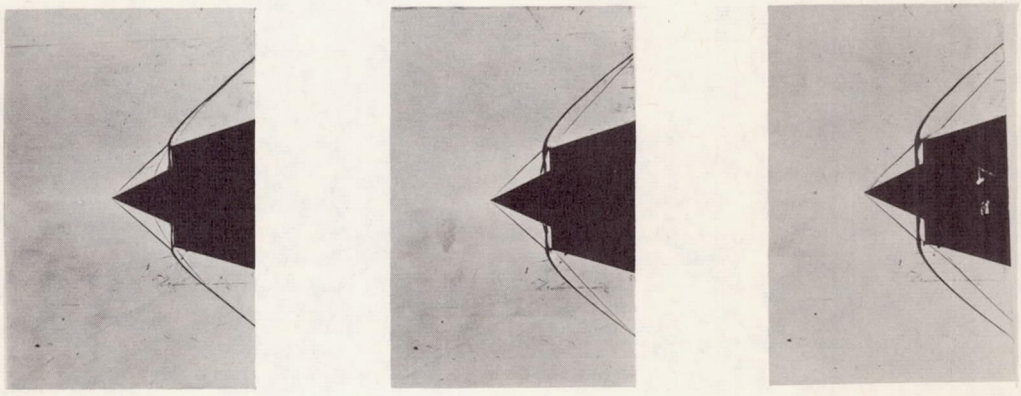


(b) Maximum pressure recovery against cowling-lip thickness.

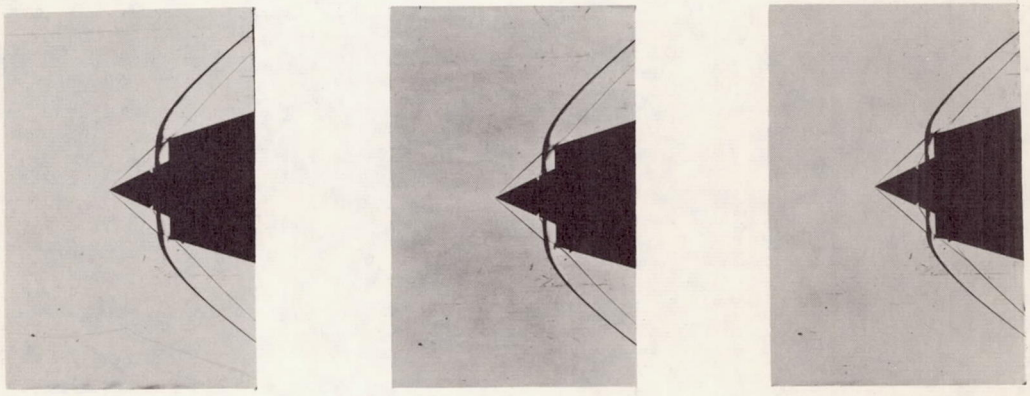
Figure 17.- Effect of cowling-lip thickness on stable mass-flow range and maximum pressure recovery for center body 1, cowling A at $\alpha = 0^\circ$.



(a) Lip thickness = 0.003 in. (b) Lip thickness = 0.010 in. (c) Lip thickness = 0.040 in.
θ_2 = 42.4°, slots open



(d) Lip thickness = 0.003 in. (e) Lip thickness = 0.010 in. (f) Lip thickness = 0.040 in.
θ_2 = 40.0°, slots closed



(g) Lip thickness = 0.003 in. (h) Lip thickness = 0.010 in. (i) Lip thickness = 0.040 in.
θ_2 = 40.0°, slots open

L-87918

Figure 18.- Shadowgraphs of minimum stable mass-flow patterns showing effect of cowling-lip thickness at an angle of attack of 0°. Center body 1 is used with variations to cowling A.